Indian Journal of Chemistry
Vol. 58A, September 2019, pp. 957-963

Decomposition and kinetics of $CH_2(OH)C(O^{\bullet})(CH_3)CH_2Cl$ radical in the atmosphere: A quantum mechanical study

Subrata Paul, Ramesh Chandra Deka* & Nand Kishor Gour*

Department of Chemical Sciences, Tezpur University Tezpur, Assam 784 028, India
Email: nkgour1@tezu.ernet.in (NKG)/ ramesh@tezu.ernet.in (RCD)

Received 11 February 2019; revised and accepted 14 August 2019

The quantum mechanical calculations of the decomposition pathways of 1, 2-hydroxy alkoxy radical i.e., $CH_2(OH)C(O^{\bullet})(CH_3)CH_2Cl$ radical have been performed. This radical species has been formed from the successive reactions with O_2 molecule and NO_x or HO_2 radicals with the most stable primary oxidation product of 3-chloro-2-methyl-1-propene and OH radical reaction. Geometry optimization and frequency calculations of all the stable species including transition states in the three possible C-C bond scission pathways (i.e., C-CH_3, C-CH_2Cl and C-CH_2OH) of $CH_2(OH)C(O^{\bullet})(CH_3)CH_2Cl$ radical have been performed at M06-2X/6-31+G(d,p) level of theory. Single point energy calculations of all the optimized species at the higher level of CCSD(T) method along with cc-pVTZ triple-zeta basis set have been performed. The rate constants for the various decomposition reactions have been evaluated using Canonical Transition State Theory (CTST) within the temperature range of 250–400 K. Rate constants for C–C bond scissions of C-CH_3, C-CH_2Cl and C-CH_2OH of the 1, 2-hydroxy alkoxy radical have been found to be 4.17×10^{1}, 1.59×10^{3} and 1.38×10^{9} s^{-1} respectively at 298 K and 1 atm. The energetic and kinetics results suggest that C–CH_2OH bond scission of titled radical has been more dominant than other decomposition channels.

Keywords: 3-chloro-2-methyl-1-propene, 1,2-hydroxy alkoxy radical, Density functinal theory, Intrinsic reaction coordinate

Unsaturated volatile organic compounds (UVOCs) are widely applicable as fuel additives or alternative fuels and halogenated solvents which lead to increase their concentration in the atmosphere[1]. These compounds are also formed in situ in the atmosphere as a result of the photo-oxidation of various hydrocarbons[1]. UVOCs undergo a number of physical and chemical processes for removal from the atmosphere or transformation in the atmosphere[1]. In the chemical process, UVOCs readily undergo primary degradation reactions with atmospheric oxidants (such as OH and NO_3 radical, Cl atom and O_3 molecule), which consequently form reactive intermediate radicals[2-4].

In literature, it is also reported that halogenated UVOCs have numerous applications ranging from industrial chemistry to laboratory synthesis[5]. After the initial reaction with OH or NO_3 radicals or Cl atoms or O_3 molecule, these halogenated UVOCs undergo secondary reaction and formed an alkyl or substituted alkyl radical (for example, hydroxyalkyl, nitrooxyalkyl or oxoalkyl radicals) in the degradation reaction mechanisms. These alkyl or substituted alkyl radicals are the key intermediates (organic peroxy ($RO_2^{\bullet}$) and alkoxy ($RO^{\bullet}$) radicals) formed by successive reacting with O_2 and NO_x (x = 1,2) molecules in the troposphere. Among the halogenated UVOCs, 3-chloro-2-methyl-1-propene (3-ClMP) is extensively used as intermediate in the synthesis of pesticides in the textile industry and as an additive in textile industry and perfume[6]. In 2015, Rivela *et al.*,[7] first study the kinetics of 3-ClMP and determined the rate constant for the reaction of 3-ClMP initiated with OH radical and Cl atoms using GC-FID techniques at 298 K and 1 atm. They found the overall rate coefficient of $(3.23 \pm 0.35)\times10^{-11}$ and $(2.10\pm0.78)\times10^{-10}$ cm^3 $molecule^{-1}$ s^{-1} for OH radical and Cl atom initiated reactions, respectively. More recently, Begum *et al.*,[8] have also investigated the OH-initiated gas phase reactions of 3-ClMP using quantum mechanical study and found the rate constant of 2.52×10^{-11} cm^3 $molecule^{-1}$ s^{-1} at 298 K. These primary reaction investigations indicate that 3-ClMP has low global warming potential and thus its contribution to the atmosphere is almost negligible. Apart from this study, it is highly necessary to investigate the decomposition reaction pathways and kinetics of alkoxy radicals (which is formed by

the secondary reaction) to understand the decomposition products.

Both experimental and theoretical primary oxidation reaction of 3-ClMP with OH radical carried out by Rivela *et al.*,[7] and Begum *et al.*,[8] showed that the primary product radical $CH_2(OH)C^{\bullet}(CH_3)CH_2Cl$ formed from the primary reaction is the most stable. In addition to that Rivela *et al.*,[7] also studied the decomposition pathway of one alkoxy radical. However, they have not provided all the possible decomposition pathways and kinetics of the $CH_2(OH)C^{\bullet}(CH_3)CH_2Cl$ radical. Thus, in this manuscript, we have carried out the quantum mechanical study on the decomposition reaction of $CH_2(OH)C(O^{\bullet})(CH_3)CH_2Cl$ radical (known as 1,2-hydroxy alkoxy radical) which is formed from product radical $CH_2(OH)C^{\bullet}(CH_3)CH_2Cl$. This 1,2-hydroxy alkoxy radical is formed by successive reactions with O_2 molecule [formed peroxy radical $CH_2(OH)C(OO^{\bullet})(CH_3)CH_2Cl$] and NO_x (x=1,2) [formed short-lived intermediate $CH_2(OH)C(OONO_2)(CH_3)CH_2Cl$] or HO_2 radicals [formed intermediate $CH_2(OH)C(OOH)(CH_3)CH_2Cl$]. These two intermediates eliminate NO_3 and OH radical and form 1,2-hydroxy alkoxy radical ($CH_2(OH)C(O^{\bullet})(CH_3)CH_2Cl$). The complete mechanism of the tropospheric degradation of $CH_2=C(CH_3)CH_2Cl$ molecule is given in Scheme 1.

In order to know the detail reaction pathways of alkoxy radical, we have performed possible decomposition pathways of the alkoxy radical. Exhaustive theoretical, as well as experimental investigations have been carried out for the decomposition of alkoxy radicals[9–13]. Alkoxy radicals play a significant role by disintegrating several types of small organic compounds and discharging into the atmosphere. Thus it justifies the investigation of the fate of 1,2-hydroxy alkoxy radical ($CH_2(OH)C(O^{\bullet})(CH_3)CH_2Cl$) from the perspective of its chemistry in the atmosphere. Theoretical study to elaborate the decomposition pathways of $CH_2(OH)C(O^{\bullet})(CH_3)CH_2Cl$ radical has so far not been carried out. The thermal decomposition of C-CH_3, C-CH_2Cl and C-CH_2Cl bonds of $CH_2(OH)C(O^{\bullet})(CH_3)CH_2Cl$ radical in the atmosphere are proceeding in the following ways:

$CH_2(OH)C(O^{\bullet})(CH_3)CH_2Cl(D)$

$CH_2(OH)C(O)CH_2Cl + C^{\bullet}H_3$ (R1)

$CH_2(OH)C(O)(CH_3)+C^{\bullet}H_2Cl$ (R2)

$CH_3C(O)CH_2Cl + C^{\bullet}H_2OH$ (R3)

Our aim is to perform the quantum mechanical calculations for the above mention decomposition pathways including transition states, thermo chemistry and kinetics. All the results are reported herein and compared our results with available experimental results.

Experimental

Computational Details and Kinetic Theory

Quantum mechanical calculations of all possible decomposition reaction channels were performed with

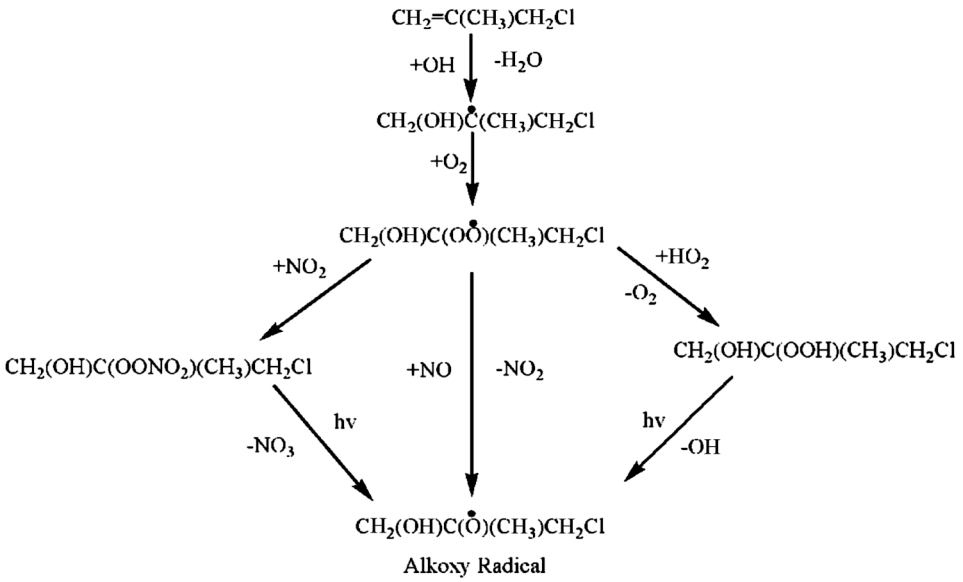

Tropospheric degradation mechanism of $CH_2=C(CH_3)CH_2Cl$ initiated by OH radicals

Scheme 1

the GAUSSIAN09 package[14]. Geometry optimization and frequency calculations of all species were performed using density functional study (DFT) employing M06-2X functional[15] with the 6-31+G(d,p) basis set. All the stationary points have been identified to be the minima with no imaginary frequency (NIMAG = 0) and the transition states with one imaginary frequency (NIMAG = 1). To ascertain the identified transition states, which truly connect the reactants and products smoothly, Intrinsic Reaction Coordinate (IRC) calculations[16] were performed at the same level of theory. Single-point energy calculations were performed at higher level of CCSD(T) method[17] along with cc-pVTZ basis set. This dual level of quantum calculations provides better energies and kinetics results in earlier theoretical studies of the abstraction and decomposition reactions[18-21]. The rate constants of decomposition reactions of $CH_2(OH)C(O^{\bullet})(CH_3)CH_2Cl$ radical is calculated using canonical transition state theory (CTST)[22] that involves a semi-classical one-dimensional multiplicative tunneling correction factor. The rate constants are computed using the following expression:

$$k = \Gamma(T)\frac{k_B T}{h}\frac{Q_{TS}^{\#}}{Q_R}\exp\frac{-\Delta E^{\#}}{RT} \quad \ldots (1)$$

where $\Gamma(T)$ is the tunneling correction factor at temperature T, $Q_{TS}{}^{\#}$ and Q_R are the total partition functions for the transition state and reactant respectively. $\Delta E^{\#}$, k_B and h are the barrier height, Boltzmann's and Planck's constants respectively. We adopted the simple and computationally inexpensive Wigner's method[23] for the estimation of the tunneling correction factor using the following expression:

$$\Gamma(T) = 1 + \frac{1}{24}\left(\frac{h\nu^{\#}}{k_B T}\right)^2 \quad \ldots (2)$$

where $\nu^{\#}$ is the imaginary frequency at the saddle point.

Results and Discussion

Optimized Structures and Frequency analysis

Optimized geometries of all the species and transition states along with the bond length (in Å) involved in decomposition reaction channels (R1-R3) carried out at M06-2X/6-31+G(d,p) level of theory are shown in Fig. 1.

In the optimized structure of TS1 for R1 reaction pathway, the elongation of the C-CH_3 bond of $CH_2(OH)C(O^{\bullet})(CH_3)CH_2Cl$ radical is found to be 2.130 Å from the equilibrium distance of 1.543 Å of C-CH_3 bond. At the same time, the C=O bond distance of TS1 decreases from 1.378 Å (equilibrium distance) to 1.236 Å. Thus, the percentage elongation of C-CH_3 and shrinkage of C=O bond are 38% and 10.3%, respectively. Similarly, in TS2 and TS3, the elongation of the C-CH_2Cl and C-CH_2COH bonds are found to be 2.087 Å and 2.129 Å from the equilibrium distances of 1.539 Å and 1.535 Å of the C-CH_2Cl and C-CH_2COH bonds of $CH_2(OH)C(O^{\bullet})(CH_3)CH_2Cl$ radical, respectively. Simultaneously, shrinkage of C=O bonds are also observed in TS2 and TS3, where C=O bonds are shrinkage to 1.249 Å and 1.244 Å with respect equilibrium C=O bond distance in TS2 and TS3, respectively. The percentage elongations of C-CH_2Cl and C-CH_2OH bond in TS2 and TS3 are found to be 35.6% and 38.7%, respectively. On the other hand, the percentage of shrinkage of C=O bond for TS2 and TS3 are 9.3% and 9.7%, respectively. The frequency calculations of all the optimized species are further performed at the same level of theory in order to obtain the various mode of vibration as well as thermochemistry of all the species. Vibration frequencies of all the species are listed in Table 1.

The stable species have real vibrational frequencies while transition states (TS1, TS2 and TS3) have only one imaginary frequency (also given in Fig. 1) as shown in Table 1. The value of the imaginary frequency of the TS1, TS2 and TS3 are **490*i*, 500*i*** and **362*i*** cm^{-1} respectively. These vibrational frequencies are analyzed using the GaussView program[24]. Visual analysis of the imaginary frequencies gives the confirmation of the presence of transition states which connecting the products and reactants qualitatively. However, it is only by intrinsic reaction coordinate (IRC) calculation that the existence of the accurate transition state on the potential energy surface is established.

Potential Energy Surface and Thermochemistry

In addition to the optimization and frequency calculations at M06-2X/6-31+G(d,p) level of theory, we have further refined the energies of all the optimized species at the higher level of coupled-

cluster CCSD(T) method using cc-pVTZ basis set. The total energy including zero-point correction of all stable species and transition states of the decomposition channels are given in Table 2 at both M06-2X/6-31+G(d,p) and CCSD(T)/cc-pVTZ//M06-2X/6-31+G(d,p) level of theories.

The energy obtained at CCSD(T)/cc-pVTZ//M06-2X/6-31+G(d,p) level of theory is higher than the energy obtained at M06-2X/6-31+G(d,p) level of theory as shown in Table 2. However, the relative energy of TSs and products with respect to $CH_2(OH)C(O^{\bullet})(CH_3)CH_2Cl$ are found to be the same trends at both the levels. A schematic two-dimensional potential energy diagram of the decomposition reaction channels (R1-R3) has been constructed with the help of total energy results (see Table 2) obtained at both levels of theories and shown in Fig. 2.

The calculated barrier heights (in kcal mol^{-1}) for TS1, TS2 and TS3 are found to be 16.17, 13.82 and 5.13 kcal mol^{-1}, respectively at CCSD(T)/cc-pVTZ//M06-2X/6-31+G(d,p) level while this these values are found to be 17.35, 15.32 and 5.59 kcal mol^{-1} at M06-2X/6-31+G(d,p) level, respectively. It is observed that C-CH_2OH decomposition (i.e., formation of TS3) followed minimum energy pathways than the formation of TS1 and TS2. Moreover, the product obtained corresponding to the TS3 i.e., P3 + CH_2OH is also most stable than others. Thus, it suggests that the decomposition channel R3 is kinetically and energetically more favorable than R1 and R2. We have also checked the nature of the

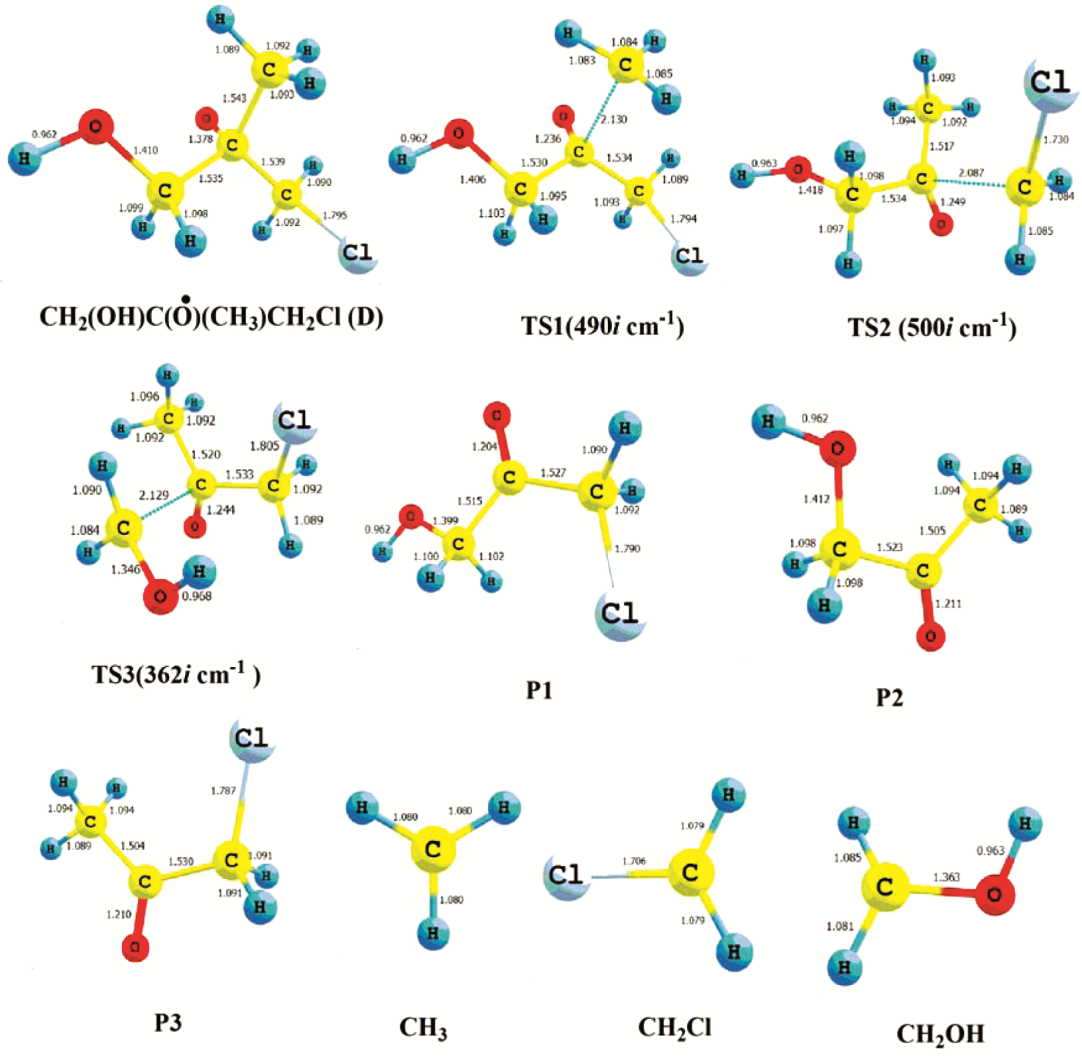

Fig. 1 — Optimized geometries of all the species along with bond length (in Å) at M06-2X/6-31+G(d,p) level of theory.

Table 1 — Vibrational frequencies of the species involved in decomposition reaction channels (R1-R3) at M06-2X/6-31+G (d, p) level of theory

Species	Vibrational frequencies (cm^{-1})
D	91, 118, 202, 239, 245, 274, 337, 355, 398, 423, 565, 740, 812, 872, 928, 963, 1000, 1089, 1141, 1168, 1193, 1244, 1290, 1298, 1331, 1391, 1444, 1481, 1487, 1507, 1523, 3047, 3087, 3100, 3118, 3174, 3191, 3207, 3927
TS1	*490i*, 56, 122, 130, 173, 217, 232, 249, 313, 414, 435, 562, 605, 633, 758, 819, 890, 969, 1030, 1129, 1172, 1206, 1225, 1274, 1299, 1426, 1439, 1452, 1469, 1514, 1625, 3018, 3110, 3117, 3119, 3203, 3289, 3304, 3923
TS2	*500i*, 80, 82, 158, 196, 219, 258, 289, 296, 402, 489, 541, 630, 767, 798, 930, 965, 1041, 1070, 1073, 1118, 1189, 1242, 1287, 1395, 1430, 1447, 1477, 1480, 1516, 1585, 3055, 3075, 3114, 3160, 3172, 3176, 3305, 3917
TS3	*362i*, 113, 124, 159, 193,237, 244, 289, 394, 429, 498, 506, 728, 742, 814, 860, 990, 1013, 1057, 1107, 1178, 1241, 1271, 1295, 1380, 1396, 1461, 1483, 1491, 1514, 1596, 3069, 3128, 3140, 3147, 3180, 3211, 3297, 3814
P1	29, 130, 179, 265, 295, 416, 456, 585, 765, 808, 862, 1027, 1145, 1190, 1195, 1239, 1271, 1300, 1451, 1457, 1490, 1887, 3029, 3068, 3122, 3194, 3923
P2	79, 159, 280, 326, 477, 499, 520, 787, 867, 991, 1097, 1141, 1199, 1259, 1276, 1397, 1430, 1464, 1472, 1493, 1865, 3054, 3075, 3100, 3146, 3202, 3920
P3	55, 143, 221, 414, 461, 494, 752, 809, 851, 994, 1047, 1210, 1256, 1305, 1396, 1448, 1462, 1470, 1864, 3074, 3124, 3147, 3190, 3198
CH_3	480, 1420, 1420, 3158, 3339, 3339
CH_2Cl	252, 834, 1014, 1440, 3222, 3376
CH_2OH	413, 644, 1057, 1245, 1349, 1502, 3158, 3302, 3917

Table 2 — Zero-point corrected total energy E_0 (Unit: Hartree) of all the species at M06-2X/6-31+G(d,p) and CCSD(T)/cc-pVTZ//M06-2X/6-31+G(d,p) level of theories

Species	Total Energy E_0 (in Hartree)	
	M06-2X/6-31+G(d,p)	CCSD(T)/cc-pVTZ//M06-2X/6-31+G(d,p)
$CH_2(OH)C(O^{\bullet})(CH_3)CH_2Cl$ (D)	–767.5418254	–766.744073
TS1	–767.5141693	–766.7183099
TS2	–767.51741	–766.7220538
TS3	–767.5329109	–766.7358833
P1 + CH_3	–767.5238656	–766.7206851
P2 + CH_2Cl	–767.5342145	–766.729206
P3 + CH_2OH	–767.5359127	–766.7439087

reaction channels (R1-R3) by calculating values of $\Delta_r H°$ and $\Delta_r G°$ at M06-2X/6-31+G(d,p) and CCSD(T)/cc-pVTZ//M06-2X/6-31+G(d,p) levels and which are reported in Table 3.

Reaction channels (R1-R3) are endothermic in nature at 298 K and 1 atm. at both levels of theories (Table 3). However, the value of $\Delta_r H°$ for R3 is 0.62 kcal mol^{-1} at CCSD(T)/cc-pVTZ//M06-2X/6-31+G(d,p) level of theory which indicates that R3 is less endothermic than R1 and R2. We further observed from the reported values of $\Delta_r G°$ of reaction channels (R1-R3) that R3 is more feasible than other channels. Thus, we can conclude from this discussion that R3 reaction channel is kinetically and thermodynamically more feasible and exothermic in nature.

Rate Constants

In view of the above discussion, the rate constant for the different C-C bond scissions (i.e., C-CH_3, C-CH_2Cl and C-CH_2OH) in $CH_2(OH)C(O^{\bullet})(CH_3)CH_2Cl$ decomposition reactions are calculated by using Eqn 1. Here, it is important to note that the value of tunnelling correction factor $\Gamma(T)$ are calculated using Wigner's method as given in Eqn 2 and are found to BE 1.23(***490*** cm^{-1}), 1.24(***500*** cm^{-1}) and 1.13(***362*** cm^{-1}) (which are almost unity) at 298 K . We have also calculated the tunneling correction factor $\Gamma(T)$ at other temperature which is also found to be unity. The calculated rate constants at M06-2X/6-31+G(d,p) and CCSD(T)/cc-pVTZ//M06-2X/6-31+G(d,p) levels for the reaction channels (R1-R3) within the temperature range of 250-400 K are reported in Table 4.

The values of the rate constant for each decomposition reaction channels are increases with the increasing temperature.(Table 4) The values of the rate constant (at 298K) for the reaction channels R1, R2 and R3 are found to be 5.63×10^{0}, 1.26×10^{2} and 6.41×10^{8} s^{-1} respectively at M06-2X/6-31+G(d,p). These values become 4.17×10^{1}, 1.59×10^{3} and 1.38×10^{9} s^{-1} respectively at CCSD(T)/cc-pVTZ//M06-2X/6-31+G (d,p) level of theory. From these kinetic results, it is found that R3 reaction channel is kinetically more dominant. Recently, Rivela *et al.*,[7] also proposed the formation of $CH_3COCH_2Cl + C^{\bullet}H_2OH$ compounds from the alkoxy radical, which is only

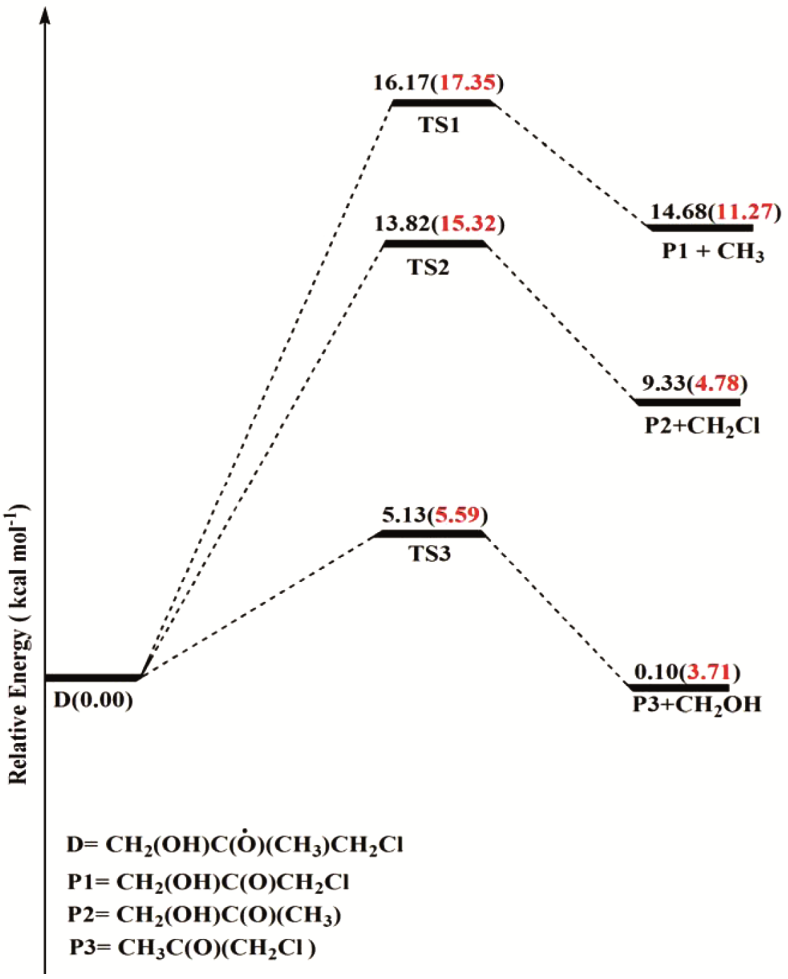

Fig. 2 — Potential energy diagram for the decomposition reactions of $CH_2(OH)C(O^{\bullet})(CH_3)CH_2Cl$ at both CCSD(T)/cc-pVTZ//M06-2X/6-31+G(d,p) and M06-2X/6 31+G(d,p) (values are in red color) level of theories.

Table 3 — Reaction enthalpy ($\Delta_rH°$) and Gibbs free energy ($\Delta_rG°$) values (in kcal mol^{-1}) for reaction channels (R1-R3) calculated at M06-2X/6-31+G(d,p) and CCSD(T)/cc-pVTZ//M06-2X/6-31+G(d,p) level of theories

Decomposition Channels	M06-2X/6-31+G(d,p)		CCSD(T)/cc-pVTZ//M06-2X/6-31+G(d,p)	
	$\Delta_rH°$	$\Delta_rG°$	$\Delta_rH°$	$\Delta_rG°$
R1	12.72	0.37	16.12	3.78
R2	5.90	-7.89	10.45	-3.34
R3	4.23	-8.02	0.62	-11.63

Table 4 — The rate constant (Unit: s^{-1}) for reaction channels (R1-R3) at M06-2X/6-31+G(d,p) and CCSD(T)/cc-pVTZ//M06-2X/6-31+G(d,p) level of theory

Rate Constant	M06-2X/6-31+G(d,p)				
	250K	298K	300K	350K	400K
k_1	1.63×10^{-2}	5.63×10^{0}	6.61×10^{0}	4.94×10^{2}	1.28×10^{4}
k_2	7.09×10^{-1}	1.26×10^{2}	1.45×10^{2}	6.66×10^{3}	1.19×10^{5}
k_3	8.64×10^{7}	6.41×10^{8}	6.77×10^{8}	3.02×10^{9}	9.43×10^{9}
	CCSD(T)/cc-pVTZ//M06-2X/6-31+G(d,p)				
k_1	1.78×10^{-1}	4.17×10^{1}	4.85×10^{1}	2.72×10^{3}	5.69×10^{4}
k_2	1.46×10^{1}	1.59×10^{3}	1.81×10^{3}	5.78×10^{4}	7.92×10^{5}
k_3	2.16×10^{8}	1.38×10^{9}	1.45×10^{9}	5.81×10^{9}	1.67×10^{10}

possible if C-CH_2OH bond scission of the 1,2-hydroxy alkoxy radical takes place. This $C^{\bullet}H_2OH$ radical further reacts with O_2 and formed HCHO and HO_2 radical. Thus our proposed reaction mechanism is in goods agreement with the reported mechanism by Rivela *et al.*[7] However, they have not reported other decomposition pathways as well as kinetics. Thus, we are unable to compare our calculated rate constant with the experimental rate constant due to lack of experimental rate constant of decomposition channels.

Conclusions

In this paper, we have presented decomposition reaction pathways and kinetics of $CH_2(OH)C(O^{\bullet})$

$(CH_3)CH_2Cl$ radical using Quantum mechanical methods. Three possible C-C (i.e., C-CH_3, C-CH_2Cl and C-CH_2OH) bond scissions of $CH_2(OH)C(O^{\bullet})(CH_3)CH_2Cl$ radical are carried out at M06-2X/6-31+G(d,p) and CCSD(T)/cc-pVTZ//M06-2X/6-31+G(d,p) level of theories. Our energetics and thermochemistry results showed that C-CH_2OH bond scission is more favorable than other decomposition channels. The kinetics results of all the three channels also suggest that the barrier height for the reaction channel R3 is lower than others. Moreover, the products $CH_3COCH_2Cl + C^{\bullet}H_2OH$ corresponding to R3 channels are more stable than other products. This detailed investigation of these decomposition reactions will be helpful for the prediction of other decomposition reaction channels which formed in the atmosphere.

Acknowledgement

Dr NKG is thankful to DST, New Delhi (Nanomission Project No. SR/NM/NS/1147/2016) for the financial assistant. One of the authors Dr S P is also thankful to the University Grant Commission (UGC), New Delhi for providing financial support from Dr D S Kothari Post-Doctoral Fellowship (Award letter no: F.4-2/2006(BSR)/CH/16-17/0152).

References

1 Atkinson R & Arey J, *Chem Rev*, 103 (2003) 4605.
2 Moortgat G, *Chemical, Physical and Biogenic Processes in the Atmosphere, COACH International Research School*, Obernai, France 2001.
3 Orlando J J, Tyndall G S, Apel E C, Riemer D D & Paulson S E, *Int J Chem Kinet*, 35 (2003) 334.
4 Finlayson-Pitts B J & Pitts Jr J N, *Chemistry of the upper and lower atmosphere: theory, experiments, and applications*, Elsevier, 1999.
5 Singh O N & Fabian P, *"Reactive bromine compounds"*. *Reactive Halogen Compounds in the Atmosphere*, Springer, Berlin, Heidelberg, 1999, pp. 1-43.
6 Mellouki A, Le Bras G & Sidebottom H, *Chem Rev*, 103 (2003) 5077.
7 Rivela C, Gibilisco R G & Teruel M A, *J Phys Org Chem*, 28 (2015) 480.
8 Begum S S, Gour N K, Baruah S D & Deka R C, *Mol Phy*, 117 (2018) 280.
9 Gour N K, Begum S S & Deka R C, *Chem Phys Lett*, 701 (2018) 157.
10 Vereecken L & Francisco J S, *Chem Soc Rev*, 41 (2012) 6259.
11 Singh H J, Mishra B K & Gour N K, *Theo Chem Acc*, 125 (2010) 57.
12 Orlando J J, Tyndall G S & Wallington T J, *Chem Rev*, 103 (2003) 4657.
13 Gour N K, Mishra B K, Sarma P J, Begum P & Deka R C, *J Flu Chem*, 204 (2017) 11.
14 Gaussian 09 Revision C. 01 (Gaussian, Inc, Wallingford CT) 2010.
15 Zhao Y & Truhlar D G, *Theo Chem Acc*, 120 (2008) 215.
16 Gonzales C & Schlegel H B, *J Chem Phys*, 95 (1991) 5853.
17 Pople J A, Head-Gordon M & Raghavachari K, *J Chem Phys*, 87 (1987) 5968.
18 Elakiya C, Shankar R, Vijayakumar S & Kolandaivel P, *Mol Phys*, 115 (2017) 895.
19 Gour N K, Rajkumari N P, Deka R C, Paul S & Deka A, *Chem Phys Lett*, 716 (2019) 35.
20 Paul S, Deka R C & Gour N K, *Env Sci Poll Res*, 25 (2018) 26144.
21 Vereecken L, Crowley J N & Amedro D, *Phys Chem Chem Phys*, 17 (2015) 28697.
22 Laidler K J, *Chemical Kinetics*, 3rd ed., Pearson Education, New Delhi, 2004.
23 Wigner E, *Z, Phys Chem*, 19 (1932) 203.
24 GaussView Version 5.0.8, Gaussian. Inc., Wallingford, CT. 2009.